Air-Coupled Ultrasound Spectroscopy Air Parameters Compensation Technique

Žilvinas Nakutis, Paulius Kaškonas, Dobilas Liaukonis, and Linas Svilainis, *Senior Member, IEEE*

***Abstract*—The air-coupled resonance ultrasound spectroscopy (RUS) of thin plate thickness, density, ultrasound velocity, and attenuation measurement is affected by air parameters. If air parameters are left unaccounted errors will occur. Conventional thermometer measurements are not efficient because temperature can vary faster than temperature sensor response. A technique for air parameters estimation and compensation of the RUS inverse solution results is proposed. The ultrasound delay over known distance is used for velocity in air estimation. There is no need for the additional measurement: the propagation time between transducers can be obtained from the RUS calibration measurement. Ultrasound velocity in air is then used for temperature estimation. These measurements are augmented by pressure sensor measurement for air density estimation. Evaluation of the attainable measurement errors and analysis of uncertainties under such compensation was carried out using simulated signals. Sensitivity coefficients for every parameter were derived and attainable errors were evaluated for the temperature range from −5 °C to +40 °C and the atmospheric pressure range from 94 to 105 kPa. It was concluded that the relative uncertainty of sample attenuation, ultrasound velocity attenuation, density, and thickness could be reduced approximately 22 times compared to the case when air parameters are assumed to be equal to those in normal conditions. Experimental verification used 2-mm polycarbonate plate, and measured values were compared against reported data. The experiment confirmed the efficiency of the proposed compensation: thickness estimation bias errors were reduced 17 times, bias errors for density were reduced 15 times, and velocity estimation bias errors were reduced 5 times.**

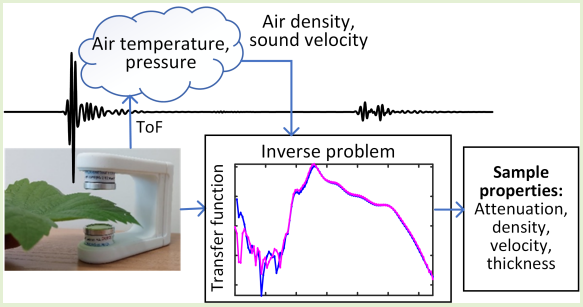

***Index Terms*— Air-coupled ultrasound, error compensation, inverse problem, plant sensor, resonance ultrasound spectroscopy (RUS), thickness and velocity measurement.**

I. Introduction

THE ultrasonic thickness gauging is a well-established technique [1], [2], [3], [4], [5], [6], [7], [8], [9], [10], [11], [12], [13], [14], [15], [16]. The principle is based on measuring the delay for ultrasonic pulse traversed the material thickness. Conventional application demands the pulse to be sufficiently narrow in order to separate the front wall and backwall reflections in time. More parameters can be measured if the test material is immersed in a fluid of known acoustic parameters. The ultrasound attenuation, velocity, density, and mechanical constants can be evaluated [2]. The thinner is the sample, and the higher should be the center frequency of the probe in order to have the required resolution. The resonance ultrasound spectroscopy (RUS) is the solution for thin plate parameters measurement [3], [4], [5], [6], [7]. While initially applied in immersion setup, later it was expanded to electromagnetic acoustic transducers (EMATs) [7], laser ultrasound [9], [10], and air-coupled ultrasound [11], [12], [13], [14]. Usually, RUS-based plate parameters estimation involves two measurements: 1) through-transmission between two transducers (addressed as calibration measurement) and 2) through-transmission between two transducers with test sample inserted (sample measurement).

New possibilities in plant science were opened once it was demonstrated that thickness resonances in the leaves could be excited and physical leaf parameters can be extracted using RUS [15], [16]. This application is of concern in this publication.

However, RUS application on leaves has a specific challenge: measurements on plants are usually carried outdoors. This means that the device has to be portable. Once addressing the problem of miniature devices [17], we have concentrated on another issue: environment conditions can differ

Manuscript received 1 November 2023; revised 14 February 2024; accepted 15 February 2024. Date of publication 29 February 2024; date of current version 16 April 2024. This work was supported by the European Regional Development Fund under Project 01.2.2-LMT-K-718-03-0026 under Grant with the Research Council of Lithuania (LMTLT). The associate editor coordinating the review of this article and approving it for publication was Dr. Marko Vauhkonen. *(Corresponding author: Žilvinas Nakutis.)*

The authors are with the Department of Electronics Engineering, Kaunas University of Technology, 53168 Kaunas, Lithuania (e-mail: zilvinas.nakutis@ktu.lt; paulius.kaskonas@ktu.lt; dobilas.liaukonis@ktu.lt; linas.svilainis@ktu.lt).

Digital Object Identifier 10.1109/JSEN.2024.3369508

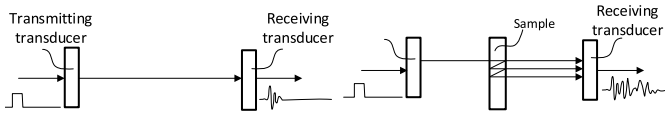

Fig. 1. RUS measurements: calibration (left) and sample (right).

significantly from those in the laboratory. In [18], it was demonstrated that disregarding the environment conditions (sound velocity in the air and air density) leads to a bias error in the leaf parameters estimation. The expected outdoor temperature variation in the range –10 °C to +40 °C and pressure variation in the range 94–105 kPa will cause −3.2% to +3.6% errors for sample thickness, −0.1% to +15.1% errors for density, and −6.8% to +6.8% errors for ultrasound velocity in the sample. There is a solution for the measurements under controlled conditions: air temperature (or even pressure) can be measured using thermometer, and then, air parameters can be estimated from such readings [19]. However, air parameters react to temperature immediately, but the thermometer reaction is slow. Therefore, even larger errors can be introduced with such a compensation. A different approach is proposed here: to measure the air parameters using an ultrasound. Ultrasound application for temperature estimation in water gives excellent precision in chemical process monitoring [20]. A similar approach can be used for oil film thickness measurement [21]. Gas thermometry is a well-known technique that estimates the temperature from the measured velocity of ultrasound [22].

It is worth noting that there is no need for additional measurement in the RUS case: the propagation delay time between transducers in calibration measurement is defined by the velocity of ultrasound in air [23], [24]; if the distance between transducers is available, the velocity of ultrasound in air can be determined. Then, the air temperature can be estimated too. Air pressure sensors are widely available and the atmospheric pressure does not vary rapidly. Air density can then be estimated using the temperature and the pressure [25]. The aim of the current work was to evaluate the attainable measurement errors under such compensation.

Section II is dedicated to the detailed description of the parameters estimation using RUS. Section III presents the research methodology. Section IV describes the finite element modeling, Section V contains the analysis of the uncertainties, and Section VI is used for experimental validation results.

II. Sample Parameters Estimation Using RUS

A typical air-coupled RUS system for the plant leaf properties measurement was reported in [17] and [18]. The sensor contains the transmitting and the receiving transducers fixed at the known distance D from each other. Two signal waveforms are acquired [12], [15], [16]: 1) calibration [no obstacle between the transducers, Fig. 1 (left)] and 2) sample [sample inserted between transducers, Fig. 1 (right)].

The spectrum of a sample signal can be expressed as a function of calibration signal [15]

$$S(\omega, \mathbf{y}, \mathbf{x}) = T(\omega, \mathbf{y}, \mathbf{x}) \cdot R(\omega) \cdot e^{j\omega \frac{h}{c_{\text{air}}}} \tag{1}$$

where $T(\omega, \mathbf{y}, \mathbf{x})$ is the transfer function dependent on the sample parameter vector $\mathbf{y}$ and the air parameter vector $\mathbf{x}$, $R(\omega)$ is the spectrum of the calibration signal received in the absence of the sample between the transducers [18], $\omega = 2\pi f$ is the angular frequency, h is the sample thickness, and c_{air} is the ultrasound velocity in the air.

Transmission of the ultrasonic signal through the sample with acoustic impedance Z_s immersed in air with impedance Z_{air} in the frequency domain is described by Brekhovskikh's model [26]

$$\mathrm{T}(\omega) = \frac{-Z_{\text{air}} Z_{\text{s}}}{-2Z_{\text{air}} Z_{\text{s}} \cos(k'h) + j\left(Z_{\text{air}}^2 + Z_{\text{s}}^2\right) \sin(k'h)} \tag{2}$$

where Z_{air} is the acoustic impedance of air, Z_s is the sample impedance, and k' is the complex wavenumber, which in turn is expressed as

$$k' = \omega / c_{\text{s}} - j\alpha \tag{3}$$

where c_s is the ultrasound velocity and α is the attenuation in a sample

$$\alpha = \alpha_0 \cdot (f/f_0)^{n_a} \tag{4}$$

where f_0 is the normalization frequency (usually center frequency of the transducer) and n_a is the power law for attenuation frequency dependence. Acoustic impedance is

$$Z_{\text{air}} = c_{\text{air}} \cdot \rho_{\text{air}},\ Z_s = c_s \cdot \rho_s \tag{5}$$

where c_{air} and c_s are the ultrasound velocity in air and sample, respectively, and ρ_{air} and ρ_s are the density of air and sample, respectively.

Referring to (2)–(5), the sample parameter vector is $\mathbf{y} = (\alpha_0, c_s\ \rho_s, h, n_a)$ and the air parameter vector is $\mathbf{x} = (c_{\text{air}}, \rho_{\text{air}})$. Parameters $\mathbf{y}$ of the sample with the unknown properties can be estimated by fitting the model (1)–(5) spectrum $S(\omega)$ to the spectrum of experimentally measured $S_E(\omega)$, assuming that the air parameter vector is $\mathbf{x}$ that is known. The optimization problem is defined as [12]

$$\begin{aligned} &\min F(\mathbf{y}, \mathbf{x}) \\ &\text{subject } \mathbf{y_{min}} < \mathbf{y} < \mathbf{y_{max}} \end{aligned} \tag{6}$$

where the objective function is

$$F(\mathbf{y}, \mathbf{x}) = |e_S| + \angle(e_S) \tag{7}$$

and

$$|e_S| = \frac{\sum_{i=1}^{N} \left(|S(\omega_i, \mathbf{y}, \mathbf{x})| - |S_E(\omega_i)|\right)^2}{\sum_{i=1}^{N} |S_E(\omega_i)|^2} \tag{8}$$

$$\angle(e_S) = \frac{\sum_{i=1}^{N} \left(\angle\{S_E(\omega_i)\} - \angle\{S_E(\omega_i)\}\right)^2}{\sum_{i=1}^{N} std\left\{\angle\{S_E(\omega_i)\}^2\right\}} \tag{9}$$

where ω_i is the ith frequency bin of the discrete Fourier transform (DFT) spectrum and N is the total number of spectrum samples.

Typical spectra of the measured and fit transmission $T(\omega)$ of grape leaf are shown in Fig. 2.

However, when the air parameters vector $\mathbf{x} = (c_{\text{air}}, \rho_{\text{air}})$, used in (6), is different from the actual air parameters vector $\mathbf{x}^* = (c_{\text{air}}^*, \rho_{\text{air}}^*)$, then the accuracy of the estimate $\mathbf{y} = (y_1, y_2, y_3, y_4, y_5) = (\alpha_0, c_s, \rho_s, h, n_a)$ degrades.

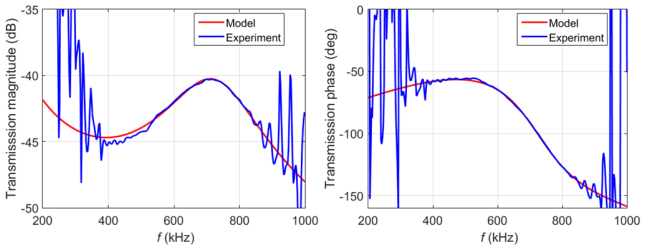

Fig. 2. Example of the typical measured and fit transmission spectra for vitis vinifera leaf.

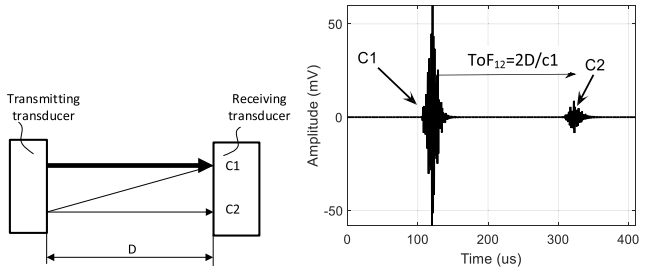

Fig. 3. Signal propagation path (left) and signal received (right) during calibration measurement.

III. Proposed Compensation Technique

Temperature, atmospheric pressure, and humidity influence ultrasound velocity in the air and density of the air. Both ultrasound velocity in the air and the air density are the input arguments to the model (1)–(5) used to estimate the sample parameters **y**. Therefore, if the ultrasound velocity in the air and the air density are not measured at the instance of calibration and sample signals acquisition, but assumed constant (usually equal to the velocity and density corresponding to normal conditions), then an error of estimation of sample parameters is introduced.

A. Ultrasound Velocity in Air Estimation

Under the assumption of dry air, the ultrasound velocity can be estimated from its temperature [33]

$$c_{\text{air}} = 20.05\sqrt{273.16 + t} \tag{10}$$

where t is the ambient temperature.

It would be natural to expect that the temperature sensor would suffice. However, any solid-state sensor (thermocouple, resistive, or semiconductor) has some inertia: temperature is reflected in the sensor only after a few minutes. On the contrary, the temperature change is immediately reflected on ultrasound velocity.

Furthermore, ultrasound velocity in air is also affected by pressure, humidity, air composition, and the excitation signal frequency [22], [23], [24], [25], [33].

Therefore, it is better to measure the ultrasound velocity, not the temperature. Time delay [time of flight (ToF)] between two transducers in calibration measurement [Fig. 1 (left)] can be used to measure the ultrasound velocity if the distance between transducers D is known. Unfortunately, ToF is also affected by delay in excitation and reception electronics and transducers. Fortunately, the calibration signal contains several signals: directly propagated signal, $C1$, and signal that reflected twice between transducers, $C2$ (see Fig. 3).

The ToF difference between these two signals is free from delay in electronics and transducers itself and is only equal to double propagation distance D delay. Then, ultrasound velocity is

$$c_{\text{air}} = \frac{2D}{\text{ToF}_{12}} \tag{11}$$

where D is the distance between transducers and ToF_{12} is the ToF between signals $C1$ and $C2$.

ToF was estimated using the cross correlation peak between signals $C2$ and $C1$. The cosine subsample interpolation was used for resolution improvement [34].

The Cramér–Rao lower error bound of ToF estimation is expected to be 0.2 ns. It was evaluated according to [34], using experimentally obtained signals. The interpolation bias error evaluated according to [35] was 0.04 ns.

Sensitivity coefficient to ToF_{12} estimation errors can be evaluated from (11) taking the derivative along ToF_{12}. For considered temperature and pressure range, it does not exceed 3.2×10^6 m/s^2, resulting in 0.0006 m/s (at 0.2 ns) velocity in air estimation error (0.0002%).

B. Distance Estimation

Several techniques can be used for distance estimation.

1) The most straightforward approach would be to measure the distance by using the caliper. An expected error would be around 100 μm.
2) If the ambient temperature is available and the temperature is stable for sufficiently long time (enough for settling time of the solid-state temperature sensor), then the distance can be estimated from ToF_{12} measurement, solving (11) for D. The velocity in such case can be estimated either using (10) or more accurate equations, presented in [23] and [36] if pressure and humidity readings are available. The expected error, assuming 1 °C temperature measurement error and 0.2-ns delay estimation error, would be around 35 μm [28].

In the actual measurement setup, transducers are attached to "U" shape holder (see insert photo along with abstract). This holder is affected by ambient temperature (expected −5 °C to +45 °C range), so distance will change due to material thermal expansion. For instance, if the holder is made from ABS (Acrylonitrile Butadiene Styrene with 100×10^{-6} m/(m·K) coefficient of thermal expansion, CTE), the distance will change by 50 μm for ±25 °C range (−5 °C to +45 °C from 20 °C nominal) when transducers' piezoelement attachment points are spaced 20 mm apart. For 30% glass fiber filled Polyamide 6-6 (CTE is 30×10^{-6} m/m/K) the distance will change by 15 μm. For aluminum (CTE is 24×10^{-6} m/m/K), change will be 12 μm. Aluminum or fiber-filled polymer is preferred for holder. In such a case, the effect of the holder thermal expansion is small.

The sensitivity coefficient for velocity in air to D estimation errors can be evaluated from (11). For considered temperature

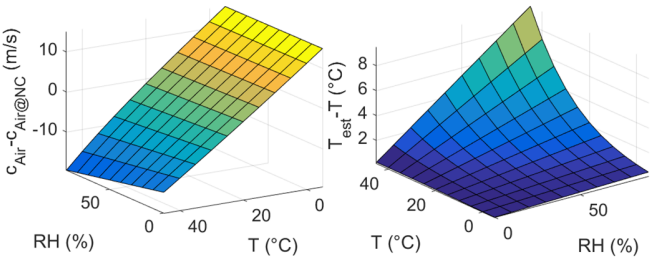

Fig. 4. Velocity in air (left) deviation from normal conditions value and ambient temperature (right) estimation errors versus temperature and humidity at 94-kPa pressure when dry air is assumed.

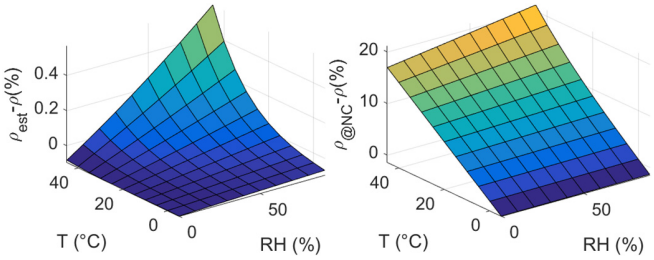

Fig. 5. Comparison of the air density estimation error versus temperature and humidity at 94-kPa pressure when the proposed technique is used for compensation (left) and uncompensated (normal conditions assumed) (right).

and pressure range, it does not exceed 18×10^3 m/s^2, resulting in 0.6 m/s (at 35-μm D estimation error) velocity in air estimation error (0.2%). With the ToF influence small, the absolute velocity in air estimation error is $\Delta(c_{\text{air}}) \leq \pm 0.6$ m/s.

C. Air Density and Temperature Estimation

The air density can be obtained from the temperature and pressure measurements using the dry air equation [33]

$$\rho_{\text{air}} = p/\left(R \cdot [273.16 + t]\right) \tag{12}$$

where t and p are the ambient temperature and atmospheric pressure, respectively, and R is the specific gas constant for dry air $R = 287.058$ J/kg·K.

The air temperature can be estimated with the ultrasound velocity and distance available. Solving (10) for temperature

$$t = (c_{\text{air}}/20.05) - 273.15. \tag{13}$$

Humidity of the air influences both ultrasound velocity in the air and air density [33], [34], [36], although to a smaller extent [see Fig. 4 (left)]. As described above, the ultrasound velocity in the air is measured using the ToF over the known distance. Yet, estimation of the temperature using dry air assumption, using (13), seems not correct because such estimation will have a bias error if there is humidity in the air. See Fig. 4 (right) for the temperature estimation error.

However, if the air density is estimated using (11), from measured pressure and temperature obtained by (13), errors are 5.7 g/m^3 (0.57%) maximum (see Fig. 5 (left) for worst case, 94-kPa pressure). Errors were estimated against velocity in air and density calculated using equations presented in [36] and [37]. If normal conditions are assumed, i.e., air parameters are not estimated and not compensated, errors reach 21%

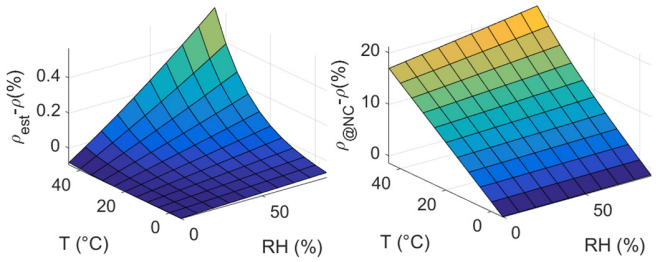

Fig. 6. Worst case (the largest distance and pressure estimation errors are included) comparison of the air density estimation error versus temperature and humidity at 94-kPa pressure when the proposed technique is used for compensation (left) and uncompensated (normal conditions assumed) (right).

[see Fig. 5 (right)]. It can be concluded that such biased temperature estimation accounts for humidity effects and air density estimation errors are small over expected temperature, pressure, and humidity range.

However, there is one more error source: pressure sensor. The atmospheric pressure P can be measured using inexpensive sensors such as BMP280 manufactured by Bosch Sensortec GmbH. The specified absolute accuracy of BMP280 after one point calibration is equal to 100 Pa over the temperature range from 0 °C to +40 °C. Fig. 6 (left) shows the worst case errors of ρ_{air} when both distance estimation and pressure estimation errors are accounted.

It can be noted that the density error is much larger when actual air parameters are not accounted [Fig. 6 (right)]. Then, the absolute error of the air density when air parameters are accounted is $\Delta(\rho_{\text{air}}) \leq \pm 10 \times 10^{-3}$ kg/m^3 and when the air parameters are not accounted is $\Delta_0(\rho_{\text{air}}) \leq \pm 210 \times 10^{-3}$ kg/m^3.

IV. Sensitivity Analysis

Sample parameters are estimated using the inverse solution of RUS, (1)–(9), and therefore, measurement equation is not available. Therefore, sensitivity coefficients cannot be obtained by differentiation. Experimental investigation can be used for sensitivities evaluation. However, it is quite complicated and time-consuming to achieve the strictly controllable ambient and sample conditions. Only one ambient parameter (temperature or pressure) should be varied with the rest remaining stable. Furthermore, the sample itself will change its parameters with temperature and pressure unpredictably, leaf parameters are changing with time and amount of light received [31]; therefore, bias error estimation becomes complicated. Therefore, it was decided to carry out the sensitivity analysis using the simulated ultrasonic signals. Such an approach enables to ensure that signals are obtained at the precisely set air temperature and pressure, in contrast to signal acquisition in the experimental setup where high-precision measurement and control of temperature and especially pressure are rather challenging.

The FEM model was implemented in OnScale Multiphysics Cloud Engineering Simulation Platform and used to synthesize calibration and sample propagated waveforms given the velocity of ultrasound in the air and the air density.

The FEM 2D-axisymetric model was used, describing two ultrasonic sensors, transmitter and receiver, placed at distance $d = 20$ mm in air medium. The PZT5A piezoceramic material of 3.15 mm thickness and 20 mm diameter was used as an active element. The backing of the sensors was made from a high-density epoxy resin, taking into account high acoustic impedance of the PZT5A. The thickness of backing layer was 6.3 mm. Three matching layers were used to achieve the acoustic impedance matching over wide frequency range between air and piezo element. Layers' acoustic impedances were calculated as given in [27].

Ricker wavelet with four subwavelets, having center frequency 650 kHz and Gaussian shape in frequency domain, was used as an excitation signal. The frequency bandwidth at −10 dB was 690 kHz. The amplitude of the excitation signal was 200 V.

Under the assumption of dry air as a medium, the parameters of air, namely, density and ultrasound wave velocity, were calculated according to (10) and (12).

The sample used typical of vitis vinifera parameters from [29], [30], and [31]: ultrasound velocity $c_s = 315$ m/s, density $\rho_s = 890$ kg/m^3, attenuation $\alpha_0 = 748$ Np/m, $n_a = 1$, and thickness $h = 0.3$ mm. The resonance frequency corresponding to this set of parameters was 525 kHz. The simulation used $-5\ ^\circ\text{C} \le t \le +40\ ^\circ\text{C}$ range of ambient air temperature and 94 kPa $\le P \le$ 105 kPa range of atmospheric pressure. Temperature and pressure in normal conditions (n.c.) were assumed at $t_{\text{nc}} = 20\ ^\circ\text{C}$ and $P_{\text{nc}} = 101.325$ kPa, respectively.

Sample parameters were estimated using simulated signals by solving the RUS inverse solution. Bias errors were obtained by subtracting the actual sample parameters from the estimated ones. The simulation environment for a sensitivity study is not important: it can be implemented in k-wave, OnScale, COMSOL, or even using (1)–(5) equations presented here; therefore, further details are not given for brevity.

A. Error Definition

Ambient temperature and atmospheric pressure influence ultrasound velocity and air density, which compose the input vector $\mathbf{x} = (c_{\text{air}}, \rho_{\text{air}})$ in the model applied in the estimation of sample properties $\mathbf{y} = (\alpha_0, c_s, \rho_s, h, n_a)$. The error vector of the sample property estimation is

$$\mathbf{e_y} = \hat{y}(\mathbf{x}) - \mathbf{y} \tag{14}$$

where $\hat{y}(\mathbf{x})$ is the RUS estimate, obtained from the calibration and sample signals by solving the inverse problem (6), and $\mathbf{y}$ is the vector of the actual sample parameters.

B. Sensitivity Coefficients Estimation

Aiming to estimate the uncertainty of $\mathbf{y}$ elements in the selected range of $\mathbf{y}$ and $\mathbf{x} = (c_{\text{air}}, \rho_{\text{air}})$ values, the linear sensitivity coefficients are required [28]. RUS results were for the $\mathbf{e_y}$ dependence on $\mathbf{e_x}$ derivation. Assuming a linear relationship between e_{yi} and e_{xi}, the influence of y_i value on e_{yi} was plotted in Figs. 7 and 8.

It can be concluded that slopes are in a linear relationship. The largest positive and least negative weights are used in uncertainty estimation aiming to characterize the worst case uncertainty.

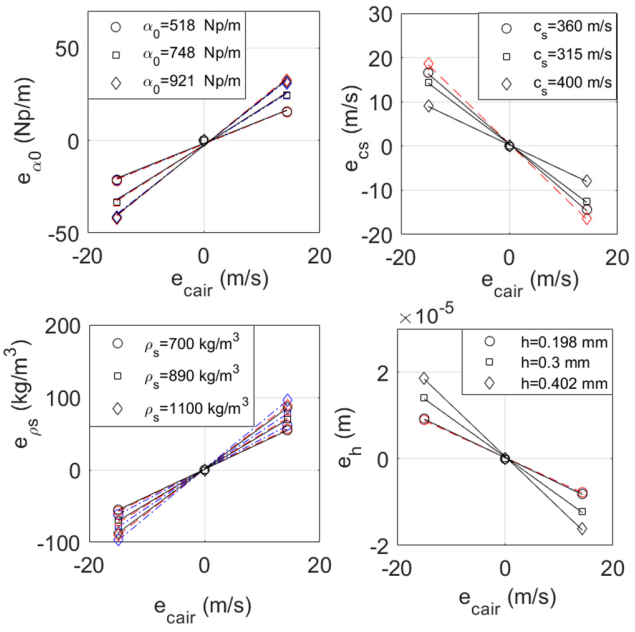

Fig. 7. Estimation error of (a) α_0, (b) c_s, (c) ρ_s, and (d) h versus c_{air} error (dashed-dotted blue line: $P = 94$ kPa, red dashed line: $P = 101$ kPa, and black solid line: $P = 105$ kPa) at three different sample parameters α_0, c_s, ρ_s, and h (nominal values are $\alpha_0 = 748$ Np/m, $c_2 = 315$ m/s, $\rho_2 = 890$ kg/m^3, and $h = 0.3$ mm).

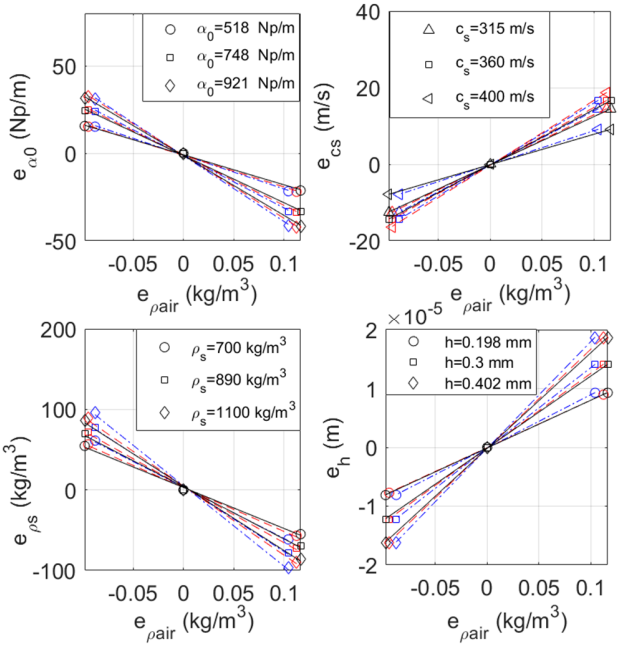

Fig. 8. Estimation error of (a) α_0, (b) c_2, (c) ρ_2, and (d) versus ρ_{air} error (at $P = 94$ kPa: dashed-dotted blue, $P = 101$ kPa: dashed red, and $P = 105$ kPa: solid black) at three different sample parameters α_0, c_s, ρ_s and h (nominal values are $\alpha_0 = 748$ Np/m, $c_2 = 315$ m/s, $\rho_2 = 890$ kg/m^3, and $h = 0.3$ mm).

The corresponding standard uncertainties of c_{air} and ρ_{air} are obtained from absolute errors derived in Section III

$$\sigma(c_{\text{air}}) = \Delta(c_{\text{air}})/\sqrt{3} = 0.35 \text{ m/s} \tag{15}$$

$$\sigma(\rho_{\text{air}}) = \Delta(\rho_{\text{air}})/\sqrt{3} = 5.77 \times 10^{-3} \text{ kg/m}^3. \tag{16}$$

TABLE I
SENSITIVITY COEFFICIENTS OF SAMPLE PARAMETERS

Parameter y_i	Sensitivity coefficients	
	c_{air}	ρ_{air}
	$w_{i1} = \partial e_{yi}/\partial e_{cair}$	$w_{i2} = \partial e_{yi}/\partial e_{\rho air}$
α_0=780 (Np/m)	2.54	-377
c_2=315 (m/s)	-1.19	169
ρ_2=890 (kg/m^3)	6.58	-1002
h =0.3 (mm)	-1.19e-6	1.81e-4

TABLE II
UNCERTAINTIES OF SAMPLE PARAMETERS ESTIMATION

y_i	Uncertainty		
	Uncompensated	*Compensated*	
	$U_0(e_{yi})$ (%)	$U(e_{yi})$ (%)	$U(e_{yi})$ (unit)
α_0=780 (Np/m)	17.1	0.78	6.06 (Np/m)
c_2=315 (m/s)	19.5	0.88	2.78 (m/s)
ρ_2=890 (kg/m^3)	1.81	1.16	16.14 (kg/m^3)
h =0.3 (mm)	21.4	0.97	2.92e-3 (mm)

These standard uncertainties and correlation coefficient $r_{12} = r(c_{\text{air}}, \rho_{\text{air}}) = -1$ referring to functional dependence (12) between c_{air} and ρ_{air} are used in the further sample properties estimation uncertainty analysis.

In case when actual air parameters are not measured, absolute errors are assumed to be equal to the minimum and maximum values over temperature and pressure range considered [refer to Fig. 4 (left) and (right)]

$$\Delta_0\left(c_{\text{air}}\right) \leq \pm 14.8 \text{ m/s}, \Delta_0\left(\rho_{\text{air}}\right) \leq \pm 210 \times 10^{-3} \text{ kg/m}^3. \tag{17}$$

Then, the corresponding standard uncertainties of c_{air} and ρ_{air}

$$\sigma_0\left(c_{\text{air}}\right) = \Delta_0\left(c_{\text{air}}\right)/\sqrt{3} = 8.5 \text{ m/s} \tag{18}$$

$$\sigma_0\left(\rho_{\text{air}}\right) = \Delta_0\left(\rho_{\text{air}}\right)/\sqrt{3} = 121 \times 10^{-3} \text{ kg/m}^3. \tag{19}$$

The sensitivity coefficients w_{ij} listed in Table I were derived numerically as relationships e_{yi} versus e_{xj} in the ranges of $\mathbf{y}$ vector elements: 581 Np/m $< \alpha_0 <$ 921 Np/m, 315 m/s $< c_2 <$ 400 m/s, 700 kg/m^3 $< \rho_2 <$ 1100 kg/m^3, and 0.198 mm $< h <$ 0.402 mm.

C. Uncertainty Estimation

According to [28] and taking into account that input quantities c_{air} and ρ_{air} are correlated, the square of combined standard uncertainty of sample property estimation is expressed

$$u^2\left(e_{y_i}, w_{ij}\right) = \sum_{j=1}^{2} w_{ij}^2 \sigma^2\left(e_{x_i}\right) + 2 w_{i1} w_{i2} r_{12} \sigma\left(e_{x_1}\right) \sigma\left(e_{x_2}\right) \tag{20}$$

where $w_{ij} = \partial e_{\text{yi}}/\partial e_{xj}$, $e_{xj} = (e_{c\text{air}}, e_{\rho\text{air}})$, and $e_{\text{yi}} = (e_{\alpha 0}, e_{cs}, e_{\rho s}, e_h)$.

The maximum standard uncertainty of the ith element $\mathbf{e_y}$ is estimated by finding the largest value according to (20)

$$u_{\max}^2\left(e_{y_i}\right) = \max\left(u^2\left(e_{y_i}, w_{ij}\right)\right), \quad j = \overline{1,2}. \tag{21}$$

Assuming a normal (Gaussian) distribution of the final quantity according to the central limit theorem, the expanded uncertainty is estimated according to expression with expansion factor 2 and coverage probability $p = 95\%$

$$U\left(e_{y_i}\right) = 2 \times u_{\max}\left(e_{y_i}\right). \tag{22}$$

The expanded standard uncertainty of sample parameters $U_0(e_{\text{yi}})$ in case when the air parameters are not estimated can be obtained from (20) to (22) by substituting $\sigma(e_{c\text{air}})$ and $\sigma(e_{\rho\text{air}})$ by $\sigma_0(e_{c\text{air}})$ and $\sigma_0(e_{\rho\text{air}})$ from (18) and (19). The uncompensated uncertainty U_0 is obtained.

The obtained uncertainties are listed in Table II.

It can be seen from Table II that the estimation of air parameters enables to reduce the maximum relative expanded uncertainty of sample properties assessed using air-coupled ultrasonic spectrometry by approximately $U_0(e_{\text{yi}})/U(e_{\text{yi}}) \approx 22$ times in the ambient parameters range $-5\ ^\circ\text{C} \leq t \leq +40\ ^\circ\text{C}$ and 94 kPa $\leq P \leq$ 105 kPa, which are typical for field applications.

V. EXPERIMENTAL VALIDATION

Experimental investigation was carried out in order to validate the suitability of the proposed compensation. The technique was initially aimed at leaf properties measurement. Unfortunately, no references exist to compare the results over the temperature range. Even simple thickness measurement using the micrometer damages the leaf. Furthermore, the leaf properties will change significantly if it is subjected to the temperature variation because of its physiology. Therefore, it was decided to use a thin polycarbonate (PC) sheet with thickness corresponding to the resonant frequency of the leaf. Sheet thickness can be measured using micrometer, it is easy to handle, and its properties have been well studied using ultrasound [38], [39], [40], [41], [42], so reference values are available.

A. Experiment Setup

The ultrasonic data acquisition system developed at Kaunas University of Technology (see insert photo at the top along with abstract) was used for signal collection. Two wideband, 650-kHz center frequency and 20-mm-diameter air-coupled ultrasonic transducers, manufactured by CSIC (Spanish Research Council, Madrid) were used for ultrasound transmission and reception. Transducers were placed at a 32-mm distance. A spread spectrum signals were used for excitation in order to keep the nonlinearity low but achieve the sufficient SNR. A 10-MHz clock frequency was used for excitation signal production. A bipolar, 32-V amplitude, 50-μs duration chirp, covering 350–950-kHz range was used for excitation. The reception gain was 8 dB for calibration and 50 dB for sample measurement. Amplifiers' complex gain ac response was measured and later used for acquired signal-level conversion to amplifier input. Signals were sampled using 14-bit, 10-MHz ADC. The detailed system description is available in [17] and [18].

Servo motor was used for automated PC plate insertion and removal for sample and calibration measurements.

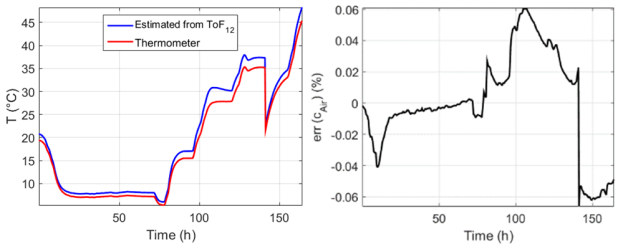

Fig. 9. Temperature profile (left) and estimated c_{air} error (right) versus time.

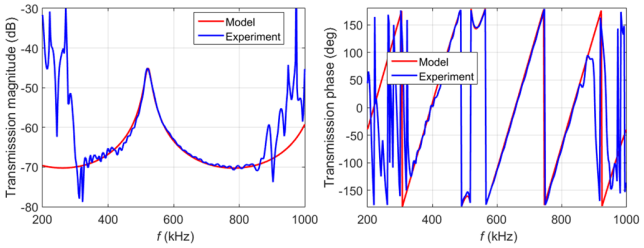

Fig. 10. Transmission response for 2-mm PC plate.

The MS8607-02BA01 sensor was used to register the ambient pressure, temperature, and humidity. Sensor pressure measurement absolute accuracy is 200 Pa, and the resolution is 1.6 Pa. Humidity is measured with 3%RH absolute accuracy, and the resolution is 0.04%RH. The temperature is measured with 1 °C absolute accuracy, and the resolution is 0.01 °C.

The whole system was placed into improvised thermal chamber. The chamber was made from the thermoelectric cooler. Temperature control was accomplished manually, by changing the cooler current. The temperature was slowly varied (approximately 1 °C/h in order to ensure the match of air and sensor temperature) from +5 °C to +40 °C. The temperature profile over experiment time is presented in Fig. 9 (left). Thermometer (red line) and ultrasound (blue line) temperature readings differ because ultrasound-estimated temperature includes relative humidity effects.

Measurement was aimed at correct ultrasound velocity estimation. Velocity in air error (difference between velocity estimated from sensor readings of P, t, and RH) profile over experiment time is presented in Fig. 9 (right).

A PC sheet of 2 mm thickness was used (supplied by Antalis, Poland, Warsaw). Transmission response for PC plate, obtained using the measured signals and provided by RUS inverse solution is presented in Fig. 10.

Comparison to Fig. 2 can reveal that transmission is smaller by 25 dB in valley, but the peak is just 5 dB lower. Signals are lower SNR than if it was leaf measurement. The resonance peak frequency is similar to that of the leaf.

B. Reference Values

The actual PC plate thickness measured by micrometer was 2.045 mm. The PC plate density was estimated, by cutting the rectangular plate and measuring its dimensions with the digital caliper (69.92 × 70.03 mm) and weighting (11.964 g). Resulting 1193.6-kg/m^3 density is close to manufacturer specified density of 1200 kg/m^3. CTE of PC (65 × 10^{-6} m/m/K)

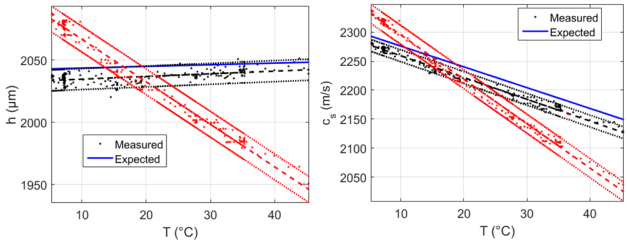

Fig. 11. Measured thickness (left) and ultrasound velocity (right) of PC plate. Red lines: uncompensated, black: compensated case, and blue line: expected values.

was used for the thickness and density change with temperature calculation. Unfortunately, ultrasonic properties usually are measured at high frequencies and therefore had to be derived from available values. Ultrasound attenuation in PC, according to [38], is 638 dB/m/MHz or 43.5 Np/m at 650 kHz. Ultrasound velocity of PC, according to [39], is 2235 m/s at 4 MHz and 2225 m/s at 1 MHz at 25 °C. It can be deduced that the velocity is 2222 m/s at 650 kHz (center frequency of the transducers used). According to [40], the ultrasound velocity is 2280 m/s, frequency not specified, but usually 5- or 10-MHz transducers are used for such measurements. Tsuji et al. [41] reported 2245-m/s velocity for PC at 15 MHz, 25 °C. Slightly different, 2192- and 2199-m/s values were reported in [42] at a 600-kHz frequency, room temperature. A negative, −3.58-m/s/°C dV/dT value for velocity change with temperature for PC was reported in [40]. It was decided to use 2240-m/s velocity at 20 °C and −3.58 m/s/°C slope in order to match the aforementioned velocity values.

Results of the PC plate thickness and velocity estimation using RUS inverse solution (red lines for uncompensated and black for compensated measurement) along with expected values (blue line) over temperature range are presented in Fig. 11. Linear regression was fit into results. Regression approximation is plotted as dashed lines, and 95% confidence intervals are indicated by dotted lines.

It can be noted that even the slope of the uncompensated measurements does not follow the physics: thermal expansion is negative. At 45 °C thickness, h is underestimated by 102 μm or 5%. At 45 °C velocity, c_s is underestimated by 124 m/s or 5.8%.

In the case of ambient parameters compensation, the slope matches the expected one. There is a slight bias error: h is underestimated by approximately 6 μm or 0.3% at 45 °C, and the bias error is reduced 17 times. At 45 °C velocity, c_s is underestimated by 23 m/s or 1.1%, and the bias error is reduced five times.

Estimated PC plate density and attenuation (red lines for uncompensated and black for compensated measurement) along with expected values (blue line) over the temperature range are presented in Fig. 12.

It can be concluded that even the slope of the uncompensated measurements does not follow the physics: density is increasing with temperature. At 45 °C air density, ρ_{air} is overestimated by 126 kg/m^3 or 11%. If ambient parameters are compensated, the slope matches the expected one. There is a slight bias error: ρ_{air} is underestimated by approximately

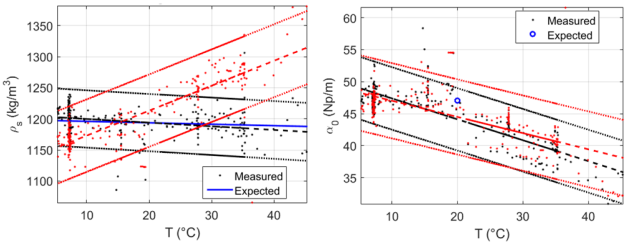

Fig. 12. Measured density (left) and ultrasound attenuation (right) of PC plate. Red lines: uncompensated, black: compensated case, and blue line: expected values.

9 kg/m^3 or 0.76% at 45 °C, and the bias error is reduced 15 times.

Attenuation α_0 can only be evaluated at 20 °C; the results are quite close for compensated and uncompensated case: approximately 2 Np/m or 4.2% was achieved.

It can be concluded that the validation experiments confirm the compensation efficiency: bias errors are reduced 17 to five times, depending on parameter.

VI. Conclusion

It was demonstrated that plate parameters (thickness, density, ultrasound velocity, and attenuation) estimation using air-coupled ultrasound resonance spectroscopy can benefit if actual air parameters (ultrasound velocity and density) are used when obtaining the inverse solution. Velocity in air and air density estimation using ultrasound and pressure sensor is proposed. It was proposed to estimate the ultrasound velocity using the ToF of probing signal's multiple reflections between transducers' surfaces. Cross correlation peak is used for ToF estimation with cosine subsample estimation. The presented sensitivity and uncertainty analysis proves that measuring the current air parameters and applying compensation in RUS should enable to noticeably improve the accuracy of estimation. Errors can be reduced approximately 22 times. Experimental validation results confirmed that compensation is possible, thickness estimation bias errors were reduced 17 times, density bias errors were reduced 15 times, and velocity estimation bias errors were reduced five times. Attenuation estimation errors did not change significantly and remained at 4.2%.

References

[1] K. A. Fowler, G. M. Elfbaum, K. A. Smith, and T. J. Nelligan, "Theory and application of precision ultrasonic thickness gauging," *Insight*, vol. 38, no. 8, pp. 582–587, Aug. 1996.

[2] J. S. Egerton, M. J. S. Lowe, P. Huthwaite, and H. V. Halai, "Ultrasonic attenuation and phase velocity of high-density polyethylene pipe material," *J. Acoust. Soc. Amer.*, vol. 141, no. 3, pp. 1535–1545, Mar. 2017, doi: 10.1121/1.4976689.

[3] W. Sachse and Y.-H. Pao, "On the determination of phase and group velocities of dispersive waves in solids," *J. Appl. Phys.*, vol. 49, no. 8, pp. 4320–4327, Aug. 1978, doi: 10.1063/1.325484.

[4] N. F. Haines, J. C. Bell, and P. J. McIntyre, "The application of broadband ultrasonic spectroscopy to the study of layered media," *J. Acoust. Soc. Amer.*, vol. 64, no. 6, pp. 1645–1651, Dec. 1978, doi: 10.1121/1.382131.

[5] R. A. Kline, "Measurement of attenuation and dispersion using an ultrasonic spectroscopy technique," *J. Acoust. Soc. Amer.*, vol. 76, no. 2, pp. 498–504, Aug. 1984, doi: 10.1121/1.391591.

[6] J. Wu, "Determination of velocity and attenuation of shear waves using ultrasonic spectroscopy," *J. Acoust. Soc. Amer.*, vol. 99, no. 5, pp. 2871–2875, May 1996, doi: 10.1121/1.414880.

[7] F. F. Balakirev, S. M. Ennaceur, R. J. Migliori, B. Maiorov, and A. Migliori, "Resonant ultrasound spectroscopy: The essential toolbox," *Rev. Sci. Instrum.*, vol. 90, no. 12, Dec. 2019, Art. no. 121401, doi: 10.1063/1.5123165.

[8] S. Dixon, C. Edwards, and S. B. Palmer, "High accuracy non-contact ultrasonic thickness gauging of aluminium sheet using electromagnetic acoustic transducers," *Ultrasonics*, vol. 39, no. 6, pp. 445–453, Oct. 2001, doi: 10.1016/s0041-624x(01)00083-x.

[9] N. Nakamura, H. Ogi, and M. Hirao, "Resonance ultrasound spectroscopy for measuring elastic constants of thin films," *Jpn. J. Appl. Phys.*, vol. 43, no. 5S, pp. 3115–3118, May 2004, doi: 10.1143/jjap.43.3115.

[10] A. Moreau et al., "On-line measurement of texture, thickness and plastic strain ratio using laser-ultrasound resonance spectroscopy," *Ultrasonics*, vol. 40, no. 10, pp. 1047–1056, Dec. 2002, doi: 10.1016/S0041-624X(02)00255-X.

[11] W. M. D. Wright and D. A. Hutchins, "Air-coupled ultrasonic testing of metals using broadband pulses in through-transmission," *Ultrasonics*, vol. 37, no. 1, pp. 19–22, Jan. 1999, doi: 10.1016/S0041-624X(98)00034-1.

[12] T. E. Gómez Álvarez-Arenas, "Simultaneous determination of the ultrasound velocity and the thickness of solid plates from the analysis of thickness resonances using air-coupled ultrasound," *Ultrasonics*, vol. 50, no. 2, pp. 104–109, Feb. 2010, doi: 10.1016/j.ultras.2009.09.009.

[13] J. Rus and C. U. Grosse, "Thickness measurement via local ultrasonic resonance spectroscopy," *Ultrasonics*, vol. 109, Jan. 2021, Art. no. 106261, doi: 10.1016/j.ultras.2020.106261.

[14] K. Bente, J. Rus, H. Mooshofer, M. Gaal, and C. U. Grosse, "Broadband air-coupled ultrasound emitter and receiver enable simultaneous measurement of thickness and speed of sound in solids," *Sensors*, vol. 23, no. 3, p. 1379, Jan. 2023, doi: 10.3390/s23031379.

[15] T. E. Gómez Álvarez-Arenas, D. Sancho-Knapik, J. J. Peguero-Pina, and E. Gil-Pelegrín, "Noncontact and noninvasive study of plant leaves using air-coupled ultrasounds," *Appl. Phys. Lett.*, vol. 95, no. 19, Nov. 2009, Art. no. 193702, doi: 10.1063/1.3263138.

[16] M. D. Fariñas, D. Sancho-Knapik, J. J. Peguero-Pina, E. Gil-Pelegrín, and T. E. G. Álvarez-Arenas, "Contact-less, non-resonant and high-frequency ultrasonic technique: Towards a universal tool for plant leaf study," *Comput. Electron. Agricult.*, vol. 199, Aug. 2022, Art. no. 107160, doi: 10.1016/j.compag.2022.107160.

[17] A. Aleksandrovas et al., "Miniature air coupled ultrasound data acquisition system for field application of resonance spectroscopy," in *Proc. IEEE Int. Ultrason. Symp. (IUS)*, Oct. 2022, pp. 1–3, doi: 10.1109/IUS54386.2022.9958013.

[18] L. Svilainis et al., "Air-coupled ultrasound resonant spectroscopy sensitivity study in plant leaf measurements," in *Proc. IEEE Sensors*, Oct. 2021, pp. 1–4, doi: 10.1109/SENSORS47087.2021.9639612.

[19] N. M. Samiudin, I. Yang, Y. T. Kim, and I. Doh, "Focused ultrasound thermometry: A two-dimensional resistance temperature detector array in a tissue-mimicking material," *IEEE Sensors J.*, vol. 21, no. 22, pp. 25624–25631, Nov. 2021, doi: 10.1109/JSEN.2021.3116589.

[20] A. N. Kalashnikov, V. Ivchenko, R. E. Challis, and A. K. Holmes, "Compensation for temperature variation in ultrasonic chemical process monitoring," in *Proc. IEEE Ultrason. Symp.*, Oct. 2005, pp. 1151–1154.

[21] Y. Jia, T. Wu, P. Dou, and M. Yu, "Temperature compensation strategy for ultrasonic-based measurement of oil film thickness," *Wear*, vol. 476, Jul. 2021, Art. no. 203640, doi: 10.1016/j.wear.2021.203640.

[22] M. R. Moldover, R. M. Gavioso, J. B. Mehl, L. Pitre, M. de Podesta, and J. T. Zhang, "Acoustic gas thermometry," *Metrologia*, vol. 51, no. 1, pp. R1–R19, Feb. 2014, doi: 10.1088/0026-1394/51/1/r1.

[23] O. Cramer, "The variation of the specific heat ratio and the speed of sound in air with temperature, pressure, humidity, and CO_2 concentration," *J. Acoust. Soc. Amer.*, vol. 93, no. 5, pp. 2510–2516, May 1993, doi: 10.1121/1.405827.

[24] K. N. Huang, C. F. Huang, Y. C. Li, and M. S. Young, "High precision, fast ultrasonic thermometer based on measurement of the speed of sound in air," *Rev. Sci. Instrum.*, vol. 73, no. 11, pp. 4022–4027, Nov. 2002, doi: 10.1063/1.1510576.

[25] A. Kon, N. Wakatsuki, and K. Mizutani, "Temperature dependence of parametric phenomenon in airborne ultrasound for temperature measurement," *Jpn. J. Appl. Phys.*, vol. 47, no. 8R, pp. 6530–6535, Aug. 2008, doi: 10.1143/jjap.47.6530.

[26] L. M. Brekhovskikh and O. A. Godin, *Acoustics of Layered Media I. Plane and Quasi-Plane Waves*. Berlin, Germany: Springer-Verlag, 1990.

[27] V. T. Rathod, "A review of acoustic impedance matching techniques for piezoelectric sensors and transducers," *Sensors*, vol. 20, no. 14, p. 4051, Jul. 2020, doi: 10.3390/s20144051.

[28] *Evaluation of Measurement Data—Guide to the Expression of Uncertainty in Measurement*, document JCGM 100:2008, Corrected version 2010, 2010.

[29] M. D. Farinas, T. E. G. Alvarez-Arenas, D. Sancho-Knapik, J. J. Peguero-Pina, and E. Gil-Pelegrin, "Shear waves in plant leaves at ultrasonic frequencies: Shear properties of vegetal tissues," in *Proc. Int. Ultrason. Symp.*, Oct. 2012, pp. 1513–1516, doi: 10.1109/ULTSYM.2012.0378.

[30] T. E. G. Álvarez-Arenas, D. Sancho-Knapik, J. J. Peguero-Pina, A. Gómez-Arroyo, and E. Gil-Pelegrín, "Non-contact ultrasonic resonant spectroscopy resolves the elastic properties of layered plant tissues," *Appl. Phys. Lett.*, vol. 113, no. 25, Dec. 2018, Art. no. 253704, doi: 10.1063/1.5064517.

[31] M. D. Fariñas, D. Sancho-Knapik, J. Peguero-Pina, E. Gil-Pelegrín, and T. E. G. Álvarez-Arenas, "Monitoring of plant light/dark cycles using air-coupled ultrasonic spectroscopy," *Phys. Proc.*, vol. 63, pp. 91–96, Jan. 2015, doi: 10.1016/j.phpro.2015.03.015.

[32] T. E. G. Alvarez-Arenas, "Acoustic impedance matching of piezoelectric transducers to the air," *IEEE Trans. Ultrason., Ferroelectr., Freq. Control*, vol. 51, no. 5, pp. 624–633, May 2004, doi: 10.1109/TUFFC.2004.1320834.

[33] A. B. Dennis, "Environmental effects on the speed of sound," *J. Audio Eng. Soc.*, vol. 36, pp. 8690–8710, Apr. 1988.

[34] L. Svilainis, "Review on time delay estimate subsample interpolation in frequency domain," *IEEE Trans. Ultrason., Ferroelectr., Freq. Control*, vol. 66, no. 11, pp. 1691–1698, Nov. 2019, doi: 10.1109/TUFFC.2019.2930661.

[35] L. Svilainis, K. Lukoseviciute, V. Dumbrava, and A. Chaziachmetovas, "Subsample interpolation bias error in time of flight estimation by direct correlation in digital domain," *Measurement*, vol. 46, no. 10, pp. 3950–3958, Dec. 2013, doi: 10.1016/j.measurement.2013.07.038.

[36] K. Rasmussen, "Calculation methods for the physical properties of air used in the calibration of microphones," Dept. Acoustic Technol., Tech. Univ. Denmark, Lyngby, Denmark, Tech. Rep. PL-11b, 1997.

[37] R. S. Davis, "Equation for the determination of the density of moist air (1981/91)," *Metrologia*, vol. 29, no. 1, pp. 67–70, Jan. 1992, doi: 10.1088/0026-1394/29/1/008.

[38] K. Ono, "A comprehensive report on ultrasonic attenuation of engineering materials, including metals, ceramics, polymers, fiber-reinforced composites, wood, and rocks," *Appl. Sci.*, vol. 10, no. 7, p. 2230, Mar. 2020, doi: 10.3390/app10072230.

[39] J. R. Asay and A. H. Guenther, "Experimental determination of ultrasonic wave velocities in plastics as functions of temperature. IV. Shear velocities in common plastics," *J. Appl. Polym. Sci.*, vol. 11, no. 7, pp. 1087–1100, Jul. 1967, doi: 10.1002/app.1967.070110708.

[40] E. Ginzel and R. Ginzel, "Approximate dV/dT values for some materials," *NDT.Net, e-J. Nondestruct. Test.*, vol. 22, no. 9, pp. 1–10, Sep. 2017.

[41] K. Tsuji, T. Norisuye, H. Nakanishi, and Q. Tran-Cong-Miyata, "Simultaneous measurements of ultrasound attenuation, phase velocity, thickness, and density spectra of polymeric sheets," *Ultrasonics*, vol. 99, Nov. 2019, Art. no. 105974, doi: 10.1016/j.ultras.2019.105974.

[42] K. A. Wear, "Measurements of phase velocity and group velocity in human calcaneus," *Ultrasound Med. Biol.*, vol. 26, no. 4, pp. 641–646, May 2000, doi: 10.1016/s0301-5629(99)00172-6.

Žilvinas Nakutis received the Ph.D. degree in measurement engineering from Kaunas University of Technology, Kaunas, Lithuania, in 2001.

Since 2015, he has been working as a full-time Professor at the Department of Electronics Engineering, Kaunas University of Technology, where he is currently with the Measurement Technologies Research Group. He has worked in the area of measurements for more than 25 years and has authored more than 30 scientific articles. His research interests include measurements in electrical power systems, smart metering, precision agriculture, and low-power embedded systems.

Paulius Kaškonas received the Ph.D. degree in measurement engineering from Kaunas University of Technology, Kaunas, Lithuania, in 2005.

Since 2006, he has been working at the Institute of Metrology, Kaunas University of Technology. The main competences are the development of unique complex high-accuracy reference measuring systems and the development of microcontroller-based embedded systems hardware and software. He has published more than 35 scientific articles. He has deep expertise in measurement and metrology fields, in measurement experiments planning, statistical analysis of obtained measurement data, solving classification/clustering tasks, and estimation of measurement uncertainty.

Dobilas Liaukonis received the master's degree from Kaunas University of Technology, Kaunas, Lithuania, in 2013.

Since 2016, he has been working as a Lecturer at the Department of Electronics Engineering, Kaunas University of Technology, where he currently works with the Signal Technologies Group. He has worked in the area of ultrasonic measurements for more than ten years. His current areas of research include nonlinear ultrasound, adhesion quality estimation, and ultrasonic signal processing.

Linas Svilainis (Senior Member, IEEE) received the Ph.D. degree from Kaunas University of Technology, Kaunas, Lithuania, in 1996.

Since 2009, he has been working as a full-time Professor at the Department of Electronics Engineering, Kaunas University of Technology, where he is a Principal Investigator of the Signal Technologies Group. He has worked in the area of ultrasonics for more than 30 years and has authored three books, more than 150 articles, and holds two patents. His current areas of research are the design and optimization of ultrasound electronics, ultrasonic signal processing, time delay [time of flight (ToF)] estimation, spread spectrum signals, air-coupled ultrasound, large-scale LED video displays, electromagnetic compatibility, and electromagnetic interference (EMI) protection of electronic systems.

Dr. Svilainis is an Associate Editor of IEEE TRANSACTIONS ON INSTRUMENTATION AND MEASUREMENT journal.